

High displacement sensitivity in asymmetric plasmonic nanostructures

Hsuan-Chi Tseng^{1,2} and Chih-Wei Chang^{1,*}

¹Center for Condensed Matter Sciences, National Taiwan University, Taipei 10617, TAIWAN

²Department of Electro-Optical Engineering, National Taipei University of Technology, Taipei 10608, TAIWAN

*cwchang137@ntu.edu.tw

Abstract: The strong couplings between two asymmetric plasmonic nanostructures can lead to ultra-sensitive optical responses when their separation changes. We employ electromagnetic numerical simulations to study the displacement sensitivity of two kinds of plasmonic systems: (1) a split-ring resonator and a metal rod; (2) two metal rods of asymmetric lengths. Structural asymmetry makes antiparallel current interactions possible and greatly enhances the sensitivity to 5%/nm for normalized frequency changes and 29%/nm for normalized transmittance changes. These are the highest displacement sensitivity among all physical systems investigated so far. In addition, we also find that these systems display a universal scaling curve independent of their shapes or dimensions. These asymmetric plasmonic nanostructures will open widespread applications from strain mapping, surface wave or heat wave imaging, optomechanical sensing, to environmental detections.

©2010 Optical Society of America

OCIS codes: (250.5403) Plasmonics; (310.6628) Subwavelength structures, nanostructures.

References and links

1. J. N. Anker, W. P. Hall, O. Lyandres, N. C. Shah, J. Zhao, and R. P. Van Duyne, "Biosensing with plasmonic nanosensors," *Nat. Mater.* **7**(6), 442–453 (2008).
2. M. E. Stewart, C. R. Anderton, L. B. Thompson, J. Maria, S. K. Gray, J. A. Rogers, and R. G. Nuzzo, "Nanostructured plasmonic sensors," *Chem. Rev.* **108**(2), 494–521 (2008).
3. A. D. McFarland, and R. P. Van Duyne, "Single silver nanoparticles as real-time optical sensors with zeptomole sensitivity," *Nano Lett.* **3**(8), 1057–1062 (2003).
4. G. Raschke, S. Brogl, A. S. Susha, A. L. Rogach, T. A. Klar, J. Feldmann, B. Fieres, N. Petkov, T. Bein, A. Nichtl, and K. Kurzinger, "Gold nanoshells improve single nanoparticle molecular sensors," *Nano Lett.* **4**(10), 1853–1857 (2004).
5. S. S. Acimović, M. P. Kreuzer, M. U. González, and R. Quidant, "Plasmon near-field coupling in metal dimers as a step toward single-molecule sensing," *ACS Nano* **3**(5), 1231–1237 (2009).
6. K. Zhang, Y. J. Xiang, X. C. Wu, L. L. Feng, W. W. He, J. B. Liu, W. Y. Zhou, and S. S. Xie, "Enhanced optical responses of Au@Pd core/shell nanobars," *Langmuir* **25**(2), 1162–1168 (2009).
7. C. Sönnichsen, B. M. Reinhard, J. Liphardt, and A. P. Alivisatos, "A molecular ruler based on plasmon coupling of single gold and silver nanoparticles," *Nat. Biotechnol.* **23**(6), 741–745 (2005).
8. G. L. Liu, Y. D. Yin, S. Kunchakarra, B. Mukherjee, D. Gerion, S. D. Jett, D. G. Bear, J. W. Gray, A. P. Alivisatos, L. P. Lee, and F. F. Chen, "A nanoplasmonic molecular ruler for measuring nuclease activity and DNA footprinting," *Nat. Nanotechnol.* **1**(1), 47–52 (2006).
9. K. H. Su, Q. H. Wei, X. Zhang, J. J. Mock, D. R. Smith, and S. Schultz, "Interparticle coupling effects on plasmon resonances of nanogold particles," *Nano Lett.* **3**(8), 1087–1090 (2003).
10. B. M. Reinhard, M. Siu, H. Agarwal, A. P. Alivisatos, and J. Liphardt, "Calibration of dynamic molecular rulers based on plasmon coupling between gold nanoparticles," *Nano Lett.* **5**(11), 2246–2252 (2005).
11. P. K. Jain, S. Eustis, and M. A. El-Sayed, "Plasmon coupling in nanorod assemblies: optical absorption, discrete dipole approximation simulation, and exciton-coupling model," *J. Phys. Chem. B* **110**(37), 18243–18253 (2006).
12. O. L. Muskens, V. Giannini, J. A. Sánchez-Gil, and J. Gómez Rivas, "Optical scattering resonances of single and coupled dimer plasmonic nanoantennas," *Opt. Express* **15**(26), 17736–17746 (2007).
13. P. K. Jain, and M. A. El-Sayed, "Noble metal nanoparticle pairs: effect of medium for enhanced nanosensing," *Nano Lett.* **8**(12), 4347–4352 (2008).
14. A. M. Funston, C. Novo, T. J. Davis, and P. Mulvaney, "Plasmon coupling of gold nanorods at short distances and in different geometries," *Nano Lett.* **9**(4), 1651–1658 (2009).
15. P. K. Jain, and M. A. El-Sayed, "Plasmonic coupling in noble metal nanostructures," *Chem. Phys. Lett.* **487**(4–6), 153–164 (2010).

16. E. Prodan, C. Radloff, N. J. Halas, and P. Nordlander, "A hybridization model for the plasmon response of complex nanostructures," *Science* **302**(5644), 419–422 (2003).
17. P. K. Jain, W. Y. Huang, and M. A. El-Sayed, "On the universal scaling behavior of the distance decay of plasmon coupling in metal nanoparticle pairs: A plasmon ruler equation," *Nano Lett.* **7**(7), 2080–2088 (2007).
18. F. J. García de Abajo, "Nonlocal Effects in the Plasmons of Strongly Interacting Nanoparticles, Dimers, and Waveguides," *J. Phys. Chem. C* **112**(46), 17983–17987 (2008).
19. P. K. Jain, and M. A. El-Sayed, "Universal scaling of plasmon coupling in metal nanostructures: extension from particle pairs to nanoshells," *Nano Lett.* **7**(9), 2854–2858 (2007).
20. C. Tabor, R. Murali, M. Mahmoud, and M. A. El-Sayed, "On the use of plasmonic nanoparticle pairs as a plasmon ruler: the dependence of the near-field dipole plasmon coupling on nanoparticle size and shape," *J. Phys. Chem. A* **113**(10), 1946–1953 (2009).
21. T. J. Davis, K. C. Vernon, and D. E. Gomez, "Designing plasmonic systems using optical coupling between nanoparticles," *Phys. Rev. B* **79**(15), 155423 (2009).
22. Due to the asymmetric structures, the choice of D is a little arbitrary here. But the universal curve does not change much even if we choose $D = L_{rod}$ for the SRR-rod systems or $D = L_{long}$ for the asymmetric-rod system.
23. P. K. Jain, and M. A. El-Sayed, "Surface plasmon resonance sensitivity of metal nanostructures: Physical basis and universal scaling in metal nanoshells," *J. Phys. Chem. C* **111**(47), 17451–17454 (2007).
24. Even if we restrict $s/D > 0.1$ to exclude any numerical errors arising from possible nonlocal effects, we obtain $A = 0.238$ and $\tau = 0.065$, which is still much more sensitive than previous results.
25. P. K. Jain, and M. A. El-Sayed, "Surface plasmon coupling and its universal size scaling in metal nanostructures of complex geometry: Elongated particle pairs and nanosphere trimers," *J. Phys. Chem. C* **112**(13), 4954–4960 (2008).
26. Here for the SRR-rod system, the frequency change is normalized to the second resonance frequency of an individual SRR and the separation is normalized to L_{rod} . For the asymmetric-rod systems, the frequency change is normalized to the resonance frequency of the short, isolated metal rod and the separation is normalized to L_{long} . Again, due to the structural asymmetry, the choices of normalization parameters are a little arbitrary. But we have found that different combinations give similar results.
27. T. Li, R. X. Ye, C. Li, H. Liu, S. M. Wang, J. X. Cao, S. N. Zhu, and X. Zhang, "Structural-configured magnetic plasmon bands in connected ring chains," *Opt. Express* **17**(14), 11486–11494 (2009).
28. H. Liu, D. A. Genov, D. M. Wu, Y. M. Liu, J. M. Steele, C. Sun, S. N. Zhu, and X. Zhang, "Magnetic plasmon propagation along a chain of connected subwavelength resonators at infrared frequencies," *Phys. Rev. Lett.* **97**(24), 243902 (2006).
29. O. Arcizet, P. F. Cohadon, T. Briant, M. Pinar, A. Heidmann, J. M. Mackowski, C. Michel, L. Pinar, O. François, and L. Rousseau, "High-sensitivity optical monitoring of a micromechanical resonator with a quantum-limited optomechanical sensor," *Phys. Rev. Lett.* **97**(13), 133601 (2006).

1. Introduction

Nanoscale metal structures enabling localized surface plasmon resonances have generated much excitement for their diverse applications in environmental sensing and chemical labeling [1,2]. In these plasmonic systems, an external light drives the collective oscillation of the conduction electrons of a metal, which results in local-field enhancements and strong scatterings around the metal structures. Because the resonance frequency is highly sensitive to the environment, these metal structures have been extensively used for detecting molecules with zeptomole sensitivity [3–6]. Furthermore, unlike organic fluorophores, these plasmonic sensors do not suffer from blinking or bleaching. Thus they can serve as nanoscale plasmonic rulers that make high-speed analyses of macromolecules possible [7,8]. In addition, due to deep subwavelength couplings between plasmonic elements, when integrating these structures with nanoelectromechanical systems (NEMS), they will enable sensitive optical detections of thermal or even quantum fluctuations. These features are believed to generate great impacts on the field of optomechanics and NEMS in the near future.

The unusual displacement sensitivity originates from the strong distance-dependent couplings between plasmonic nanostructures. Recently, intensive works have been devoted to studies of interactions between nanorods, nanospheres, nanoshells and nano-prisms etc. with symmetric structures [9–15]. In general, the effects can be qualitatively understood by a plasmon hybridization model which considers electric interactions between plasmonic metal structures similar to chemical bonding in natural molecules [16]. The model depicts a universal scaling curve for normalized resonance frequency changes with respect to normalized distances [17]. However, so far these investigations are limited to structurally symmetric systems and it is not known which kinds of systems would exhibit the highest sensitivity. Here we show that introducing structural asymmetry makes antiparallel current interactions possible and greatly enhances the displacement sensitivity in two kinds of

plasmonic nanostructures. In fact, these two systems display the highest displacement sensitivity among all systems (including plasmonic or non-plasmonic systems) investigated so far. These structurally-asymmetric plasmonic systems, though they are fixed to a substrate, will have potential applications in strain mapping, surface wave or heat wave imaging, and thermal or quantum vibrational sensing when they are integrated with NEMS devices.

2. Methods

Figure 1 illustrates the schematics of two kinds of asymmetric plasmonic nanostructures: one consisting of a split-ring resonator (SRR) and a metal rod (Fig. 1(a)) and the other one consisting of two metal rods of asymmetric lengths (Fig. 1(b)). Since both SRRs and metal rods are model plasmonic elements which exhibit strong electric dipolar resonances, we choose these two structures for studying the effects from structural asymmetry. When the two plasmonic elements are coupled, the resonant frequency changes in accord with the coupling strength. Introducing structural asymmetry makes the interactions between each element more intriguing and may bring more interesting phenomena. To explore their potential applications in displacement sensing, we have performed numerical simulations using software package CST Microwave Studio to study the optical transmission spectra when the separation between the elements changes. We have also systematically varied the dimensions of the elements so that the resonance frequencies are within infrared to visible range for practical applications. To avoid non-local effects at small distances, we have restricted the separation (s) to be larger than 2nm [18]. The substrate is either glass (refraction index = 1.5) or sapphire (refraction index = 1.7). The dimensions of the systems are subwavelength ($\sim\lambda/4$) and couplings between nearest neighbor elements can be neglected. The electrical conductivity of gold is described by the Drude model with plasmon frequency 1.37×10^{16} Hz. Importantly, in order to consider experimental implementations, we set the damping rate of gold to be 1.2×10^{14} Hz, which is three times higher than the bulk value and is a practical parameter for experiments utilizing ordinary fabrication techniques [9,10,17]. In the simulation, a transient pulse polarized along y -axis was incident to the system and then the transmittance of the wave was analyzed. Each mesh size was less than $\lambda/2000$ to ensure simulation accuracy.

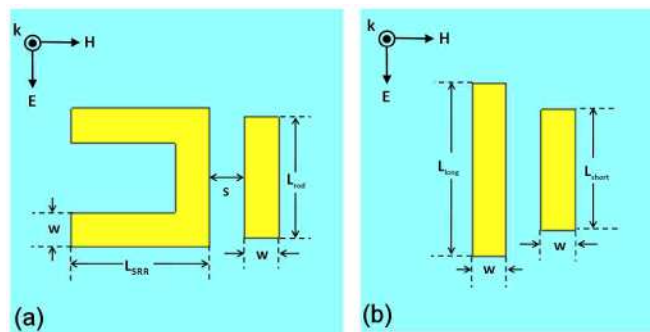


Fig. 1. Schematics of two asymmetric plasmonic nanostructures (a) a SRR and a metal rod (b) two metal rods of asymmetric lengths. An external light polarized along y -axis is incident normal to the two nanostructures. In the paper, thickness (t) = 30 nm and w = 50 nm unless otherwise mentioned.

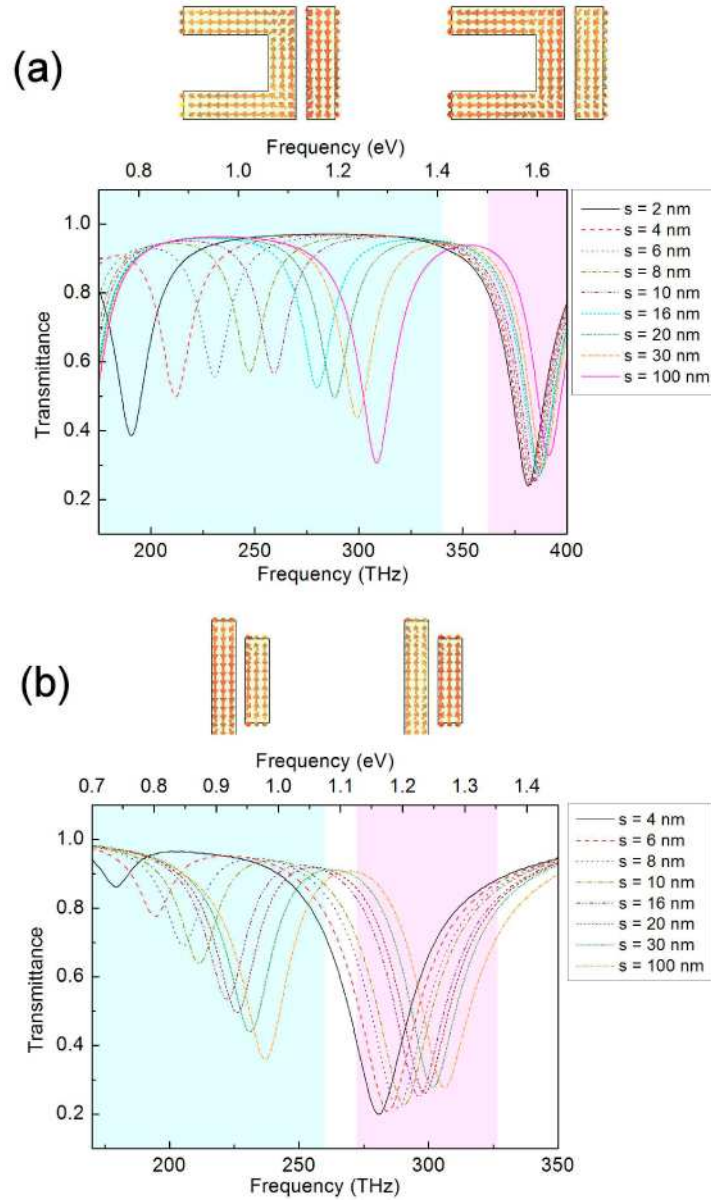


Fig. 2. Simulated separation dependent transmittance of (a) a SRR and a metal rod with $L_{\text{SRR}} = L_{\text{rod}} = 200$ nm, $t = 40$ nm, and a glass substrate, in which two resonances (as marked by the shaded blue and pink colors) are found to red-shift when reducing the separation. The upper figures display the respective current flow distributions. (b) two metal rods with $L_{\text{long}} = 250$ nm, $L_{\text{short}} = 175$ nm, and a sapphire substrate, in which two resonances (as marked by the shaded green and pink colors) are found to red-shift when reducing the separation. The upper figures display the respective current flow distributions.

3. Results and discussions

Figure 2(a) shows the simulated transmittance spectra for the SRR-rod system shown in Fig. 1(a). In the frequency range of interests, the SRR exhibits an electric dipolar resonance at 391 THz (identified by the dip of the transmittance) and the metal rod exhibits an electric dipolar resonance at 310 THz. Due to the conservation of degrees of freedom and the structural asymmetry, coupling these two elements results in two resonances which are both optically

bright modes as shown in Fig. 2(a). Interestingly, both resonances display red-shifts when the distance between the SRR and the metal rod decreases. We found the most dramatic changes to be the first resonance in the range of 180-330 THz. As shown in Fig. 2(a), the first resonance changes 68 THz when the separation slightly increases from 2 nm to 10 nm. In contrast, the second resonance (in the range of 381 THz to 385 THz) does not show such a dramatic effect. The origin of the difference can be understood from the current flow distributions for the two resonances. As shown in Fig. 2(a), the first resonance exhibits antiparallel current flows in the region of proximity. On the other hand, the second resonance, which displays small frequency changes, exhibits parallel current distributions in the region of proximity.

Similarly, coupling a long metal rod (resonance frequency = 237 THz) and a short metal rod (resonance frequency = 306 THz) results in two optically bright resonances. As shown in Fig. 2(b), the two resonances show red-shifts when the distance between the two metal rods decreases. The most dramatic change of the resonance frequency is again found in the first resonance (frequency changes 32 THz from 4 nm to 10 nm), in which the current flow shows antiparallel distributions. On the other hand, the second resonance, which exhibits parallel current distributions, only shows small changes.

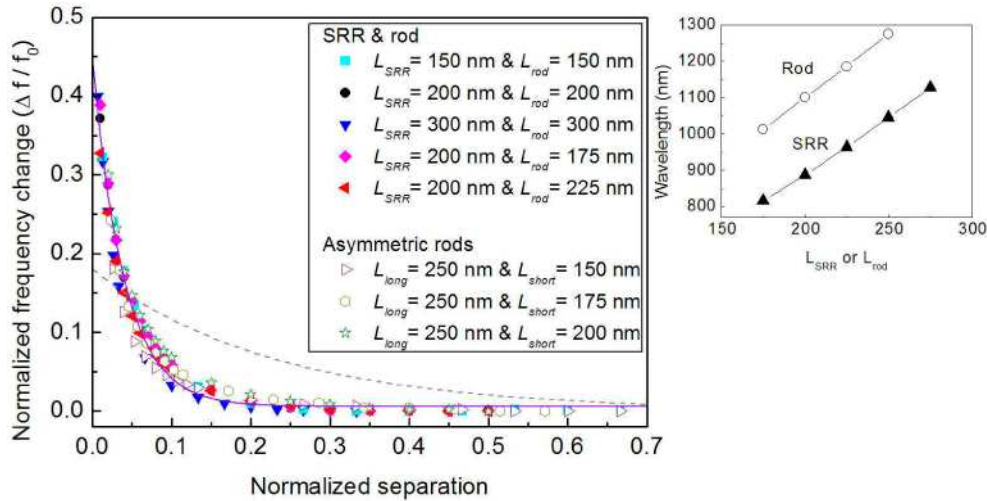


Fig. 3. (Left) Normalized frequency changes vs. normalized separations for various asymmetric nanostructures with antiparallel current interactions. For comparison, the dash line shows the universal scaling curve for a pair of nanospheres with structural (mirror) symmetry. (Right) Resonance wavelength vs. different L_{SRR} or L_{rod} , displaying a scaling relation.

A scaling relation between the resonance wavelength and the dimension of uncoupled plasmonic structures has been observed in various plasmonic systems. We have also observed the same effect shown in the right panel of Fig. 3. When the plasmonic elements are coupled, previous studies of surface plasmon resonances of a pair of nanoparticles have suggested a universal scaling curve for nanoparticles of different dimensions [19]. It is found that the curve of normalized frequency change vs. normalized separation displays a universal exponential decay with the decay length independent of the dimension of the nanoparticle but sensitive to the shape [20]. However, the universality is only examined in systems exhibiting structural (mirror) symmetry such as a pair of two identical nanodisks, nanospheres, nanoprisms or nanocubes [20]. Furthermore, although couplings between two asymmetric metal rods have been studied before, no attempt was tried to analyze their universality [21]. To investigate the scaling universality of these structurally asymmetric systems of different dimensions, we have plotted the normalized frequency changes vs. the normalized separation in Fig. 3. Remarkably, we find that all the data from different systems with antiparallel current distributions can be described by a universal exponential function, i.e:

$$\frac{\Delta f}{f_0} \approx A e^{-(s/D)/\tau} \quad (1)$$

where f_0 is the resonance frequency at $s = \infty$ and D is a normalization parameter for separation. For the SRR-rod systems, f_0 is the resonance frequency of an individual metal rod and $D = L_{SRR}$. For the asymmetric-rod systems, f_0 is the resonance frequency of the individual long metal rod and $D = L_{short}$ [22]. From the fitting curve, we obtain $A = 0.46$ and $\tau = 0.034$ for the SRR-rod and asymmetric rods systems with antiparallel current distributions. Comparing with the universal plasmon equation ($\tau = 0.18$ to 0.37) obtained from structurally symmetric plasmonic nanoparticles [17,20,23], we conclude that structural asymmetry makes antiparallel interactions possible, which greatly enhances the displacement sensitivity [24]. In fact, the highest displacement sensitivity is found in the first resonance of a SRR-rod system with $L_{SRR} = 200$ nm and $L_{rod} = 175$ nm, in which the normalized frequency change can reach 5%/nm. The highest sensitivity found in the present systems is at least two times higher than those found in nanoparticle pairs and 25% higher than the highest sensitivity reported in nanoshell pairs [19,20,25]. Importantly, the present systems can be fabricated using top-down approaches and thus will not encounter device integration problems like those of nanoshells.

On the other hand, parallel current interactions shown in the second resonance of the SRR-rod system or the asymmetric rod system do not exhibit comparable displacement sensitivities. As shown in Fig. 4, increasing the asymmetry of the SRR-rod or the asymmetric-rod systems shifts the curves upward [26]. However, the displacement sensitivities remain at least three times lower than those shown in Fig. 3.

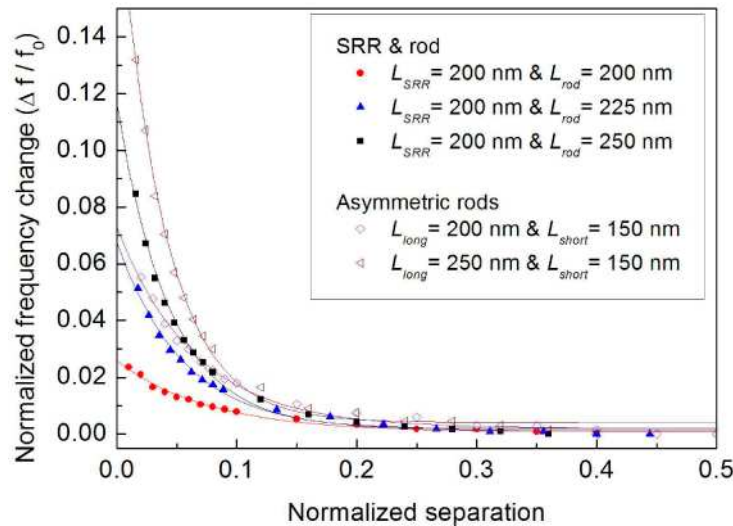


Fig. 4. Normalized frequency changes vs. normalized separations for various asymmetric nanostructures with parallel current interactions. Introducing more asymmetry into the systems shifts the curves upward but the displacement sensitivity remains low.

What can we learn from the high displacement sensitivity and the universal scaling curve? Apparently, antiparallel current interactions are the key factor for enhancing the displacement sensitivity. Furthermore, the universal scaling curve shown in Fig. 3 suggests that the underlying phenomena for antiparallel current interactions must be the same. To achieve high displacement sensitivity, it is important to note that the universal curve is plotted for $\Delta f/f_0$ vs. s/D , whereas the displacement sensitivity is defined by the ratio of $\Delta f/f_0$ to Δs . Thus the displacement sensitivity may not be the same for different plasmonic nanostructures of different dimensions. As a guideline, we find that decreasing the resonance frequencies of the whole system always results in higher displacement sensitivities. It can be achieved by decreasing the thickness of the metal or changing the substrate with a larger the refraction

index. On the other hand, changing the resonance frequency of one plasmonic unit alone affects the system in a complex way and does not always enhance the displacement sensitivity. Furthermore, it is interesting to note that previous studies on structurally symmetric plasmonic systems display blueshifts when their mutual distance decreases; whereas in Fig. 2 both resonances show redshifts. Indeed, we have observed similar blueshifts on the second resonance (i.e. the symmetric mode) once the resonance frequencies of the two plasmonic elements are identical (for example, when $L_{SRR} = 200$ nm, $L_{rod} = 150$ nm, $w = 50$ nm, and $t = 30$ nm, both the SRR and the metal rod exhibit identical resonances at 391 THz). Nevertheless, when the two resonances frequencies are not identical, the observed high displacement sensitivity at the antiparallel current distributions and the unusual redshifts at the parallel current distributions merit an explanation. Here we employ Lagrangian formalism to analyze the resonances of the structurally asymmetric plasmonic nanostructures. We have generalized the formalism in Ref [27], to incorporate the conditions due to structural asymmetry. In general, the Lagrangian of the coupled plasmonic system can be written as:

$$\mathfrak{L} = \frac{1}{2}L_1\dot{Q}_1^2 + \frac{1}{2}L_2\dot{Q}_2^2 - \frac{1}{2}L_1\omega_1^2Q_1^2 - \frac{1}{2}L_2\omega_2^2Q_2^2 + \frac{1}{2}L'(\dot{Q}_1 - \dot{Q}_2)^2 - M_m\dot{Q}_1\dot{Q}_2 - M_e\omega_1\omega_2Q_1Q_2 \quad (2)$$

where L_1, L_2 are the inductance, Q_1, Q_2 are the charges, ω_1, ω_2 are resonance frequencies of individual plasmonic units. L', M_m, M_e are respectively the community inductance, the magnetic coupling, and the electric coupling between the plasmonic units and they are all functions of s . Although the exact functional form of L', M_m, M_e are complex and cannot be given using the Lagrangian formalism alone, we know they are independent of the modes of resonances and are fixed once s is unchanged. Thus they are effective in giving quantitative results when comparing decoupled and coupled plasmonic systems. Note that the community inductance (L') in the fifth term of Eq. (2), a common term in analyzing various kinds of plasmonic or metamaterial systems [27,28], always reduces the total energy and thus contributes a redshift. On the other hand, the magnetic or the electric coupling may contribute either a redshift or a blueshift depending on the symmetric mode or the antisymmetric mode. After substituting $Q_i = A_i \exp(i\omega t)$ to the Euler-Lagrangian equation, we then have two coupled equations:

$$\begin{cases} \left[-(L_1 + L')\omega^2 + L_1\omega_1^2 \right] A_1 + \left[(L' + M_m)\omega^2 + M_e\omega_1\omega_2 \right] A_2 = 0 \\ \left[(L' + M_m)\omega^2 + M_e\omega_1\omega_2 \right] A_1 + \left[-(L_2 + L')\omega^2 + L_2\omega_2^2 \right] A_2 = 0 \end{cases} \quad (3)$$

The two eigenvalues and eigenmodes can be solved accordingly and their changes with respective to the coupling strengths can also be analyzed.

When the system is structurally symmetric ($\omega_1 = \omega_2, Q_1 = Q_2$), the fifth term of Eq. (2) is negligible and the frequency shifts mainly result from the electric and the magnetic couplings. Thus blueshifts are expected in the symmetric mode. When the system is asymmetric ($\omega_1 \neq \omega_2, Q_1 \neq Q_2$), the fifth term of Eq. (2) contribute a redshift, which competes with the electric and the magnetic couplings in the symmetric mode. Apparently, the community inductance is much stronger than the capacitor couplings in our systems so that omnipresent redshifts are observed in these structurally asymmetric plasmonic systems. In our systems, the parameters in Eq. (3) can be approximately related to a structural-asymmetry factor ($\eta = L_{long}/L_{short} = L_1/L_2$). Taking Fig. 2(b) ($\omega_1 = 237$ THz, $\omega_2 = 306$ THz, $\eta = 1.43$) for example, we find that choosing $L'/L_1 = 0.56$, $M_m/L_1 = 0.21$, and $M_e/L_1 = -0.18$ can quantitatively describe the redshifts in Fig. 2(b) and the same parameters reproduce the expected blueshifts for the symmetric mode when $\omega_1 = \omega_2$. Similar methods can be employed for analyzing Fig. 2(a) or other systems, too.

For the antisymmetric mode (antiparallel current distribution), the effect of the community inductance, the electric coupling, and the magnetic coupling contribute coherently to the large redshift. The deep subwavelength nature of these couplings, when combined with the large redshift, results in a much larger displacement sensitivity in the antiparallel current

distributions than that in the parallel current distributions. The parameters for Fig. 2(b) shown above have also quantitatively explained the main features observed in the simulation.

Although the systems investigated so far are fixed to a substrate, they can be used for strain mapping when a stress is applied to the substrate. Besides, due to the broadband optical responses, they can be used for dynamical imaging of surface waves or heat currents that produce lattice compression or refraction index changes. Moreover, once they are integrated with NEMS devices, they are also capable of detecting tiny motions arising from thermal or quantum fluctuations. For comparison, so far the highest displacement sensitivity was reported in a micromechanical resonator which incorporates a very high finesse ($F = 30000$) Fabry-Perot cavity. The device had achieved quantum-limited sensitivity at the $10^{-19} \text{m}/\sqrt{\text{Hz}}$ level [29]. Following $2\pi s/\lambda = 2/\sqrt{\mathfrak{F}}$, a displacement of $s = 2 \text{ nm}$ in the microresonator would correspond to 50% change of the transmittance at $\lambda = 1064 \text{ nm}$; or equivalently, a normalized transmittance change of 25%/nm. For our system, a monolayer of the asymmetric nanostructures can further enhance the normalized transmittance change to 29%/nm at $\lambda = 1550 \text{ nm}$. We believe that once multilayers of such asymmetric nanostructures are fabricated, more improvements can be achieved. In addition, unlike a Fabry-Perot cavity that requires multi-wavelength engineering, the plasmonic systems can further reduce the size of a device to deep subwavelength. The structurally asymmetric plasmonic systems not only exhibit the highest displacement sensitivity among all plasmonic or non-plasmonic systems investigated so far, but also can generate great impacts on nanoscale optomechanical applications. Finally, it should be noted that other varieties of asymmetric plasmonic nanostructures could exhibit even higher sensitivities. The optimization of structural designs for achieving the highest displacement sensitivity is certainly worth future investigations.

In summary, we have investigated displacement sensitivities of two kinds of structurally asymmetric plasmonic systems. The structural asymmetry makes the antiparallel current interactions possible, which greatly enhances the displacement sensitivity to reach a normalized frequency change of 5%/nm or a normalized transmittance change of 29%/nm. These structurally asymmetric plasmonic systems constitute the highest displacement sensitivity investigated so far and will have widespread applications ranging from strain mapping, surface wave or heat wave imaging, to thermal or quantum motional sensing when integrated with NEMS devices.

Acknowledgments

The authors thank Prof. W. K. Hung and Wei-Chih Ho for their helps during the early stage of the work. C. W. Chang would like to thank supports from Golden-Jade fellow of Kenda Foundation, Taiwan. This work was supported by the National Science Council of Taiwan (NSC98-2112-M-002-021-MY3).